Improved Tableting Properties of *p*-Hydroxybenzoic Acid by Water of Crystallization: A Molecular Insight

Changquan (Calvin) Sun[1,2,3] and David J. W. Grant[1]

Received February 7, 2003; accepted June 12, 2003

Purpose. To understand the influence of water in the crystal structure on the compaction properties of otherwise structurally similar crystals, *p*-hydroxybenzoic acid anhydrate (HA) and the monohydrate (HM) were used as model compounds.

Methods. Bulk powder of HM was prepared by exposing HA powder to 97% relative humidity at 23°C. Each powder, HA or HM, was uniaxially compressed and triaxially decompressed under various pressures to form square-faced tablets. The tensile strength and porosity of the tablets were measured.

Results. Incorporation of water into the crystal lattice results in greater tablet strength and larger reduction in volume for HM crystals than for HA crystals. Both HA and HM crystals contain hydrogen-bonded, zigzag-shaped layers that lie parallel to the (401) plane. When HA crystals are compressed, the zigzag-shaped layers mechanically interlock, inhibiting slip and reducing plasticity. However, water molecules in the HM crystals assume a space-filling role, which increases the separation of the layers. This effect allows easier slip between layers and provides greater plasticity of HM crystals, which increases the interparticulate bonding area under the same compaction pressure. However, the water molecules in the HM crystals increase their lattice energy by forming a three-dimensional hydrogen-bonding network. The greater bonding strength that results is reflected in greater tensile strength of HM compacts at zero porosity.

Conclusions. The presence of water molecules in the crystal structure of *p*-hydroxybenzoic acid facilitates plastic deformation of HM crystals, thereby enhancing their bonding strength and giving much stronger tablets than of HA crystals.

KEY WORDS: hydrate; *p*-hydroxybenzoic acid; plasticity; slip planes; tableting.

INTRODUCTION

The incorporation of water molecules into the lattice of drug crystals may alter pharmaceutically important properties such as solubility and tableting behavior (1). Although reports of thermodynamics and kinetics of hydrated systems abound (2–4), relatively few have touched on the effects of water of crystallization on mechanical properties (5,6). Consequently, the influence of water of crystallization on the tableting performance of powders remains to be evaluated case by case, such that no reliable prediction of tableting performance is yet possible. The objective of this work is to explain at the molecular level the effects of water of crystallization on the tableting properties of crystals in powder form.

[1] Department of Pharmaceutics, College of Pharmacy, University of Minnesota, Weaver-Densford Hall, 308 Harvard Street S.E., Minneapolis, MN 55455-0343.

[2] Present address: Pharmacia Corporation, 7000 Portage Road, Portage MI 49001.

[3] To whom correspondence should be addressed (email: changquan.sun@pharmacia.com).

The differences in the tableting performance of sulfamerazine polymorphs in powder form has been explained by differences in their crystal structures, specifically by the slip planes in Form I and their absence in Form II (7). The slip planes in polymorph I provide greater plastic deformation of the particles during compaction, which favors the formation of tablets that are stronger for Form I than for Form II (7). To understand further the relationship between slip planes and tableting performance, we compare here the tableting performance of anhydrate and monohydrate crystals of *p*-hydroxybenzoic acid. The results suggest that the water of crystallization in crystals of *p*-hydroxybenzoic acid monohydrate acts as a lubricant that facilitates easier plastic deformation of hydrate crystals than of anhydrate crystals, thereby conferring better tableting performance.

MATERIALS AND METHODS

Materials

p-Hydroxybenzoic acid anhydrate (HA) in powder form (Sigma Chemical Co., St. Louis, MO) was used as received. To prepare *p*-hydroxybenzoic acid monohydrate (HM), HA in powder form (250 g) was stored over saturated potassium nitrate solution at 94% relative humidity (RH) for 2 months at 23°C. Powder X-ray diffractometry (PXRD) and Karl Fischer titrimetry (KFT) confirmed complete conversion of HA to HM under the above conditions. For each HA and HM powder, the fraction passing through a 595-μm sieve but retained by a 350-μm sieve was collected and was stored as a thin layer on a sheet of aluminum foil for 24 h in an environmentally controlled room at 60 ± 2% RH and at 25°C. This treatment was intended to reduce the difference in surface moisture between the HA and HM powders. At the above RH and temperature, both HA and HM are kinetically stable for at least 1 week. Microscopic observation showed that particles in both HA and HM powders exhibited essentially the same morphology and size. Therefore, the influence of particle size and morphology on tableting performance was minimized in this study.

Experimental Methods

Karl Fischer Titrimetry (KFT)

The water content of HA and HM powders was determined by KFT using a Moisture Meter (model CA-05, Mitsubishi Chemical Industries Ltd., Tokyo, Japan). Samples (6–7 mg) were accurately weighed and quickly transferred to a titration vessel to minimize the uptake of atmospheric moisture. Pure, dry methanol was used as the solvent. The water contents (w/w) were: HA measured 0.02 ± 0.03% (n = 3, HA theoretical 0%); HM measured 11.58 ± 0.08% (n = 3, HM theoretical 11.54%).

True Density Measurements

The true density, ρ_t, of the powders (Table I) was determined in triplicate using a helium pycnometer (model 1320, Micromeritics, Norcross, GA). The pycnometer was calibrated daily using a steel ball of standard size.

0724-8741/04/0200-0382/0 © 2004 Plenum Publishing Corporation

Table I. Particulate and Mechanical Properties of *p*-Hydroxybenzoic Acid Anhydrate (HA) and Monohydrate (HM) in Powder Form (Sieve Fraction 350–595 μm)

Crystal form	True density (g/cm^3) measured[a]	True density (g/cm^3) calculated[b]	σ_0 (MPa)[c]	b[d]
Anhydrate	1.454 (0.003)	1.497	3.62[e]	9.31[e]
Monohydrate	1.770 (0.060)	1.398	11.75[f]	9.23[f]
			5.35[g]	3.83[g]

[a] Measured using helium pycnometry, which causes dehydration of HM. Standard deviations are stated in parentheses, $n = 3$.
[b] Calculated from the crystal structures (references 8, 9).
[c] σ_0 is the tensile strength, σ, extrapolated to zero porosity, in Eq. (1), $n = 3$.
[d] b is the exponential constant in Eq. (1), $n = 3$.
[e] From regression of data for the porosity values, 0.1–0.4, $R^2 = 1.00$, $n = 3$.
[f] From regression of data for the porosity values, 0.17–0.4, $R^2 = 0.99$, $n = 3$.
[g] From regression of data for the porosity values, <0.2, $R^2 = 0.97$, $n = 3$.

Preparation of Tablets

Powders of suitable weight were compressed under a hydraulic press (Carver, model C, Menomonee, WI) at various compaction pressures in a split die, which allowed uniaxial compression and triaxial decompression to make square-faced tablets of dimension 19 mm × 19 mm × 8 mm. Before each compaction, the punches and die were lubricated with a 5% (w/v) suspension of magnesium stearate in ethanol and were dried. The compaction pressure ranged from 10.4 MPa to 200 MPa, and the dwell time was 1 min. All tablets were allowed to relax for 24 h in an environmentally controlled room at 60 ± 2% RH and at 25°C before subsequent measurements of dimensions and tensile strength. The dimensions of the tablets were measured to ± 0.02 mm using a dial caliper (Mitutoyo Manufacturing Co., Japan). Hence, the volume of each compact was calculated. The porosities of tablets were calculated from the true density of the powder, the weight, and the volume of the tablets. The tensile strength of the tablets was determined in triplicate using a compressive test procedure (7).

X-Ray Diffractometry

Powder X-ray diffraction (PXRD) patterns of compacts or powders were collected using an X-ray diffractometer (Siemens, model D5005, Germany) with Cu Kα radiation generated at 40 mA and 45 kV. Counts were measured using a scintillation counter. Each powder was packed into a sample holder and was pressed by a clean glass slide to ensure coplanarity of the powder surface with the surface of the holder. To determine its PXRD pattern, a square-faced tablet was mounted on a small piece of modeling clay, placed at the bottom of a deeper holder, and was gently pressed down, using a flat glass slide, until the surface of the tablet was coplanar with the surface of the holder. The scans were run from 5° to 35° 2θ in increments of 0.05° with a counting time of 3 s for each step. To identify the solid phases, the experimental PXRD patterns were compared with the theoretical patterns calculated from crystal structures of HA and HM.

The PXRD pattern of a mixture of 2% (w/w) HA + 98% (w/w) HM revealed the characteristic peak of HA at 14.7° 2θ. Therefore, the detection limit of HA in the powder mixture was 2% (w/w) or less. Similarly, the detection limit of HM in powder mixtures was also found to be 2% (w/w) or less because the characteristic peak of HM at 17.65° 2θ was observed in the PXRD pattern of the powder mixture containing 2% (w/w) HM.

Crystal Structures and Molecular Modeling

The crystal structures of HA and HM were downloaded from the Cambridge Structural Database (8,9), using commercial software (Graphic QUEST3D, Cambridge Crystallographic Data Center, 1995). The crystal lattice structures of HA and HM were visualized using commercial software (Material Studio, Accelrys, San Diego, CA). The theoretical PXRD patterns of HA and HM were calculated and were used as a reference for identification of the solid phase.

RESULTS AND DISCUSSION

True Density Measurement

The measured true density of HM was greater than that calculated from crystallographic data (Table I), perhaps because of dehydration of HM during true density measurements where the samples were held in an atmosphere of dry helium. About 1.5% weight loss of HM samples after true density measurements supported this suggestion. We therefore used the true density value derived from crystal structural data to calculate tablet porosity at room temperature. The crystal structure of HM was solved from X-ray diffraction data collected at 22°C (8). When the experimental PXRD pattern of HM was compared with the PXRD pattern calculated from the single crystal structure, no peak shift was observed, indicating no significant lattice expansion. The calculated true density of HM (1.398 g/cm^3) agrees with the true density measured by the flotation method (1.398 g/cm^3) (8). The measured true density of HA was slightly lower than the calculated value (Table I), perhaps because of imperfections in the crystals in HA powder. The measured true density was used for subsequent calculation of the porosity of HA tablets.

Relationship Between Compaction Pressure and Tensile Strength

The tensile strength of tablets of both HA and HM increases with increasing compaction pressure (Fig. 1). The tensile strength increases more rapidly for HM and almost linearly at compaction pressures lower than 60 MPa (Fig. 1). At the same compaction pressure, HM always forms stronger tablets than HA (Fig. 1), indicating the superior tabletability of HM. Therefore, the presence of water molecules in *p*-hydroxybenzoic acid crystals improves tableting performance.

The difference between the tensile strength values of HA and HM may be attributed to either different interparticular bonding areas or different bonding strengths or both. However, it is generally not possible to identify the reasons for the better tableting performance of HM over HA without considering tablet porosity. A plot of porosity vs. compaction pressure (Fig. 2) provides information on compressibility (volume reduction under pressure), and a plot of tensile

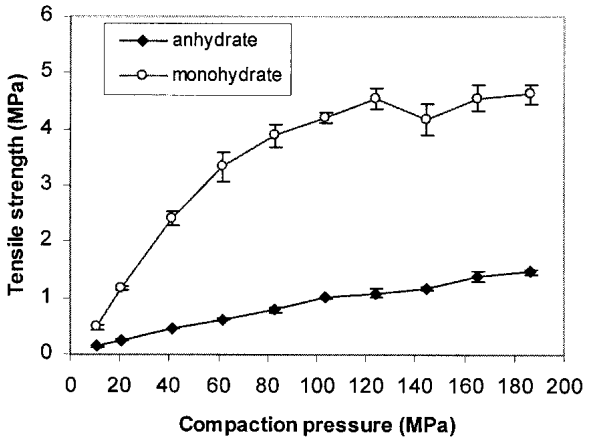

Fig. 1. Plots of tensile strength against compaction pressure, showing greater strength of tablets prepared from *p*-hydroxybenzoic acid monohydrate (HM) powder than from *p*-hydroxybenzoic anhydrate (HA) powder.

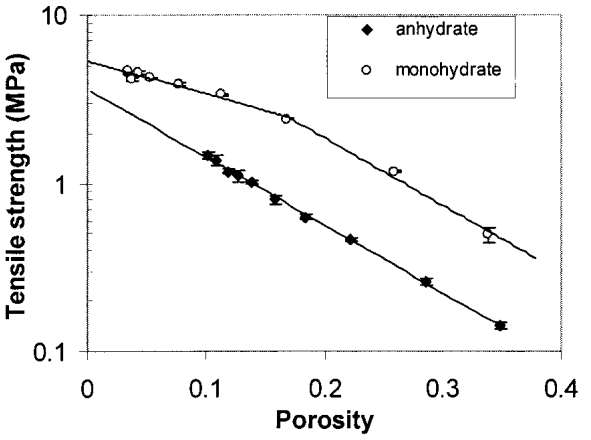

Fig. 3. Plots of tensile strength against tablet porosity, showing greater tablet strength of *p*-hydroxybenzoic acid monohydrate (HM) powder than of *p*-hydroxybenzoic acid (HA) powder from porosity 0.10 to 0.35.

strength vs. porosity (Fig. 3) provides information on compactibility (bonding strength normalized by porosity) (10–12). In the PXRD pattern of compressed HM tablets, the characteristic peaks of HA were not detected. Therefore, compaction itself did not induce detectable dehydration of HM crystals.

Relationship Between Porosity and Compaction Pressure

For both HA and HM powders, porosity decreases with increasing compaction pressure (Fig. 2), indicating the effect of compaction pressure on consolidation. At the same pressure, the porosity of HM tablets is always significantly lower than that of HA tablets, indicating that HM is more easily consolidated. Volume reduction of a powder may be achieved through particle rearrangement, fragmentation of particles, and plastic deformation (13). For both HA and HM the similar porosity at about 10 MPa rules out more extensive particle rearrangement of HM. The similarity of the mean particle sizes and morphologies of the two powders explain this result.

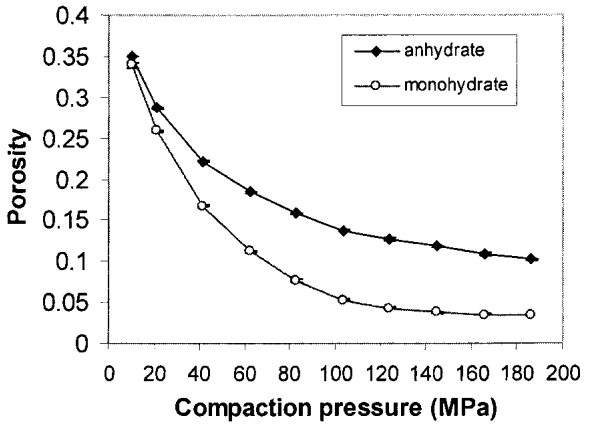

Fig. 2. Plots of tablet porosity against compaction pressure. Lower porosity of *p*-hydroxybenzoic acid monohydrate (HM) tablets indicates greater compressibility and easier consolidation of HM powder than of *p*-hydroxybenzoic acid anhydrate (HA) powder. The similar tablet porosity at the lowest pressure (10 MPa) indicates that the initial packing of the particles is similar for the two powders.

Relationship Between Porosity and Tensile Strength

The tensile strength, σ, of porous tablets made from HA decreases exponentially with increasing porosity, ε (Fig. 3), according to Eq. (1) by Ryshkewitch (14).

$$\sigma = \sigma_0 \, e^{-b\varepsilon} \tag{1}$$

where σ_o is the tensile strength of the tablet extrapolated to zero porosity, and b is a constant that may be linked to the pore distribution within a tablet (12,15). When pores are not homogeneously distributed in a tablet, reduction of tablet porosity by compression will likely be achieved through shrinkage of large pores and elimination of the smallest pores. Consequently, reduction of porosity by this mechanism may be expected to increase the overall tablet strength to a greater extent than by homogeneous shrinkage of pores of similar size. As a result, the slope of the plot of $\ln(\sigma)$ vs. porosity is greater, corresponding to a higher b value. The plot of $\ln(\sigma)$ against porosity for HM appears bilinear (Fig. 3). The exact mechanism for this behavior is under investigation. We propose that the change of slope may reflect a change of consolidation mechanism of HM at higher pressures.

The preexponential factor b is the same for HA and HM at porosity 0.2–0.4 (Table I), indicating that the initial pore distribution is similar for HA and HM tablets. Similar pore structure is expected during the initial compression of HA and HM powders because of the similarities in their initial particle size and shape. However, at a higher pressure, corresponding to a lower porosity, the shape and size of pores, and hence the bonding area at a given porosity, will differ between HA and HM tablets. This difference may be attributed to the differences in plasticity between HA and HM crystals.

Under low pressure, HM crystals undergo particle rearrangement, fragmentation, and plastic deformation, with the former two mechanisms dominating the consolidation process. Elastic deformation of the particles is reversible and does not contribute to their permanent deformation. Under higher pressures, at which particle rearrangement and fragmentation are reduced, plastic deformation is the dominating mechanism of the irreversible change of the HM crystals.

Therefore, at the same porosity, the shapes of pores, and consequently the interparticulate bonding area, will differ from those for which the deformation mechanism of HM is assumed not to change. On the other hand, HA crystals may still undergo fragmentation and particle rearrangement, even at the highest compaction pressure, at which the tablet porosity, 0.10, is substantially higher than 0.03 for HM tablets when compressed at the same pressure (Fig. 2). Consequently, the plot of ln(σ) against porosity for HM gives a different slope. At any given porosity from 0.35 to 0.10, Fig. 3 also shows that the tensile strength of HM tablets is much greater than that of HA tablets, indicating the greater lattice energy of HA crystals. This observation accords with the fact that the dehydration reaction is endothermic (9).

Relationship Between the Crystal Structures and Tableting Performance

Table II compares the crystallographic data of HA and HM crystals. Analysis of the crystal structures of HA and HM reveals a similar layered structure in both crystals, as shown in Fig. 4. In HA crystals, two *p*-hydroxybenzoic acid molecules are hydrogen bonded (O-O distance 2.635 Å) through two carboxyl groups to form a dimer. These dimers are held together by hydrogen bonds (O-O distance 2.897 Å) between the phenolic groups to form layers of two-dimensional hydrogen-bonding networks that are parallel to the (401) plane (Fig. 4a,b). In HM crystals, hydrogen-bonded dimers of *p*-hydroxybenzoic acid molecules (O-O distance 2.658 Å) are similarly held together by hydrogen bonds between the phenolic hydroxyl groups and water molecules (O-O distance 2.603 Å) to form layers. Each layer consists of an infinite two-dimensional network that is also parallel to the (401) plane (Fig. 4c,d). In addition, the layers are linked together by hydrogen bonds between the carbonyl oxygens and water molecules (O-O distance 2.827 Å) to form a three-dimensional network.

Because the three-dimensional hydrogen-bonding network in HM crystals results in a more rigid crystal lattice that lessens fragmentation, the possibility of more extensive fragmentation of HM crystals can also be ruled out. Therefore, the better consolidation of HM (Fig. 2) is attributed to its superior plasticity. Because reduced porosity normally results in a larger interparticulate bonding area, the better tabletability of HM may be attributed, at least partially, to its superior plasticity.

During compaction of HA crystals, the zigzag-shaped layers are capable of being compressed by the resolved components of the normal pressure (Fig. 5). If we treat the compaction process under a Carver press as a pseudoequilibrium process, the van der Waals force between the layers should compensate for the external compression force that is applied to each crystal. As a result, layers in HA crystals are compressed close to each other before significant slip occurs (Fig. 5). Subsequent plastic deformation through slip between layers is more difficult because the relative movement between the layers requires displacement of the molecules from their equilibrium positions. Displacement of molecules in turn necessitates breakage of the intermolecular hydrogen bonds and overcoming the van der Waals forces.

Table II. Crystallographic Information for *p*-Hydroxybenzoic Acid Anhydrate (HA) and Monohydrate (HM)[8,9]

	Anhydrate	Monohydrate
Crystal class	Monoclinic	Monoclinic
Z	4	4
Space group	$P2_1/a$	$P2_1/a$
a (Å)	18.508 (7)	17.752 (9)
b (Å)	5.228 (2)	6.442 (2)
c (Å)	6.342 (3)	6.731 (3)
β (°)	93.22 (3)	105.48 (6)

Standard deviations are stated in parentheses.

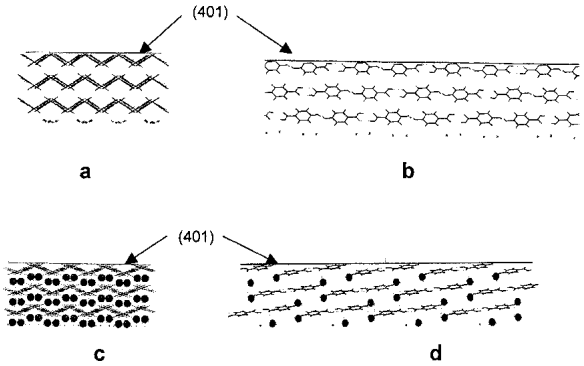

Fig. 4. Crystal structures of *p*-hydroxybenzoic acid anhydrate (HA) and monohydrate (HM). Both structures show zigzag-shaped layers of hydrogen-bonded two-dimensional networks parallel to the (401) plane. (a) HA crystal structure viewed along the ⟨–4 0 1⟩ direction; (b) HA crystal structure viewed along ⟨0 1 0⟩; (c) HM crystal structure viewed along ⟨–4 0 1⟩; (d) HM crystal structure viewed along ⟨0 1 0⟩. The solid spheres represent oxygen atoms of water molecules in the HM crystal. The broken lines represent hydrogen bonds.

In HM crystals, water molecules reside between molecular layers (Fig. 4c,d). Water molecules fill the spaces between the *p*-hydroxybenzoic acid molecules, which are organized in a way that provides layers of smoother surfaces than in HA crystals (Fig. 4). Moreover, during the compaction process, the water molecules between layers in HM crystals assure only a small reduction of interlayer distance under a normal stress. Therefore, a smoother surface and a larger spacing between the layers facilitate slip between the layers during compression (Fig. 5). In order for two neighboring layers to slide over each other, only the hydrogen bond (O-O distance 2.827 Å) that connects the layers needs to be broken by shear stress. The relatively long oxygen–oxygen distance of this hydrogen bond indicates a relatively weak interaction between the water molecules and the *p*-hydroxybenzoic acid molecules. For typical O-H···O hydrogen bonds, the O–O distance ranges from 2.5 Å to 2.8 Å (16). Moreover, because slip normally occurs through movement of dislocations in a crystal, only one hydrogen bond at a time needs to be disturbed to allow plastic deformation within the crystals. Hence, the water molecules facilitate plastic deformation of HM crystals. A macroscopic analogy of the process is the reduction of friction between surfaces by a lubricant.

CONCLUSIONS

This study explains the difference in tableting performance between *p*-hydroxybenzoic acid anhydrate (HA) and the monohydrate (HM), which have similar crystal structures.

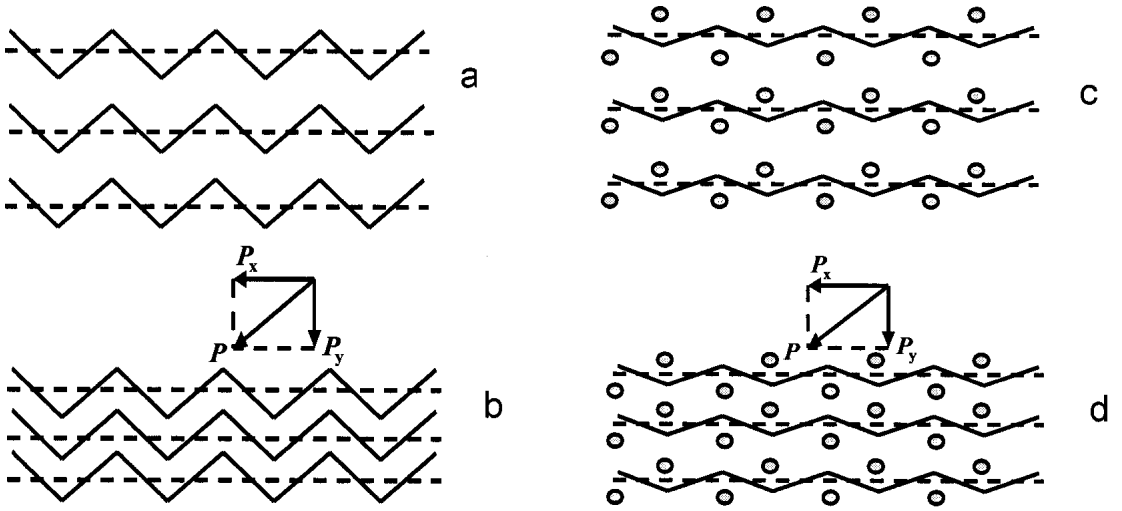

Fig. 5. Illustration of the response of crystals under external mechanical stress, P, which is resolved into shear stress, P_x, and normal stress, P_y: (a) *p*-hydroxybenzoic acid anhydrate (HA) crystal unstressed; (b) HA crystal under compressive stress; (c) *p*-hydroxybenzoic acid monohydrate (HM) unstressed; (d) HM crystals under compressive stress. Water molecules maintain separation between layers, thereby allowing easier slip.

Zigzag-shaped layers of two-dimensionally hydrogen-bonded *p*-hydroxybenzoic acid molecules lie parallel to the (401) planes in both crystals. In the HM crystal, water molecules fill the space between the layers. The presence of water molecules in the crystal structure of HM facilitates plastic deformation of the crystals by maintaining a larger separation between the zigzag-shaped (401) planes to permit easier slip under pressure. Consequently, HM crystals have greater plasticity, and HM tablets have a larger interparticulate bonding area. Water molecules in HM crystals are also hydrogen-bonded to *p*-hydroxybenzoic acid molecules to form a three-dimensional network. Thus, the presence of water molecules in the crystal also enhances the bonding strength of HM. The combination of larger interparticulate bonding area and higher bonding strength within HM tablets results in the superior tableting properties of HM over HA.

ACKNOWLEDGMENTS

We thank the American Foundation for Pharmaceutical Education (AFPE) for the award of a Fellowship to one of the authors (C.S.). We thank Pharmacia Corporation for use of the commercial software (Material Studio, Accelrys, San Diego, CA) and the data station. We also thank the Supercomputer Institute of the University of Minnesota for supporting our use of the Medicinal Chemistry/Supercomputing Institute Visualization Workshop Laboratory.

REFERENCES

1. R. K. Khankari and D. J. W. Grant. Pharmaceutical hydrates. *Thermochim. Acta* **248**:61–79 (1995).
2. E. Shefter and T. Higuchi. Dissolution behavior of crystalline solvated and nonsolvated forms of some pharmaceuticals. *J. Pharm. Sci.* **52**:781–791 (1963).
3. S. Petit and G. Coquerel. Mechanism of several solid-solid transformations between dihydrated and anhydrous copper(II) 8-hydroxyquinolinates. Proposition for a unified model for the dehydration of molecular crystals. *Chem. Mater.* **8**:2247–2258 (1996).
4. H. Zhu, C. Yuen, and D. J. W. Grant. Influence of water activity in organic solvent + water mixtures on the nature of the crystallizing drug phase. 1. Theophylline. *Int. J. Pharm.* **135**:151–160 (1996).
5. C. F. Lerk, K. Zuurman, and K. Kussendrager. Effect of dehydration on the binding capacity of particulate hydrates. *J. Pharm. Pharmacol.* **36**:399 (1983).
6. D. Y. T. Wong, P. Wright, and M. E. Aulton. The deformation of alpha-lactose monohydrate and anhydrous alpha-lactose monocrystals. *Drug Dev. Ind. Pharm.* **14**:2109–2126 (1988).
7. C. Sun and D. J. W. Grant. Influence of crystal structure on the tableting properties of sulfamerazine polymorphs. *Pharm. Res.* **18**:274–280 (2001).
8. M. Colapietro, A. Domenicano, and C. Marciante. Structural studies of benzene derivatives. VI. Refinement of the crystal structure of *p*-hydroxybenzoic acid monohydrate. *Acta Crystallogr.* **B35**:2177–2180 (1979).
9. E. A. Heath, P. Singh, and Y. Ebisuzaki. Structure of *p*-hydroxybenzoic acid and *p*-hydroxybenzoic acid–acetone complex (2/1). *Acta Crystallogr.* **C48**:1960–1965 (1992).
10. E. Joiris, P. D. Martino, C. Berneron, A.-M. Guyot-Hermann, and J.-C. Guyot. Compression behavior of orthorhombic paracetamol. *Pharm. Res.* **15**:1122–1130 (1998).
11. C. Sun and D. J. W. Grant. Compaction properties of L-lysine salts. *Pharm. Res.* **18**:281–286 (2001).
12. C. Sun and D. J. W. Grant. Effects of initial particle size on the tableting properties of L-lysine monohydrochloride dihydrate powder. *Int. J. Pharm.* **215**:221–228 (2001).
13. P. E. Wray. The physics of tablet compaction revisited. *Drug Dev. Ind. Pharm.* **18**:627–658 (1992).
14. E. Ryshkewitch. Compression strength of porous sintered alumina and ziroconia. *J. Am. Cer. Soc.* **36**:65–68 (1953).
15. R. J. Robert, R. C. Rowe, and P. York. The relationship between the fracture properties, tensile strength, and critical stress intensity factor of organic solids and their molecular structure. *Int. J. Pharm.* **125**:157–162 (1995).
16. L. Pauling. *The Nature of the Chemical Bond and the Structure of Molecules and Crystals: An Introduction to Modern Structural Chemistry*, 3rd ed. Cornell University Press: New York, 1960, pp. 484–485.